PII: S0032-3861(96)00639-8

Polymer Vol. 38 No. 6, pp. 1273–1283, 1997

0032-3861/97/$17.00+0.00

Morphological studies of binary homopolymer/block copolymer blends: effect of molecular weight

Chureerat Prahsarn and Alexander M. Jamieson*
Department of Macromolecular Science, Case Western Reserve University, Cleveland, OH 44106, USA
(Received 7 February 1996; revised 28 May 1996)

Morphological investigations of solvent-cast polymer blend films, containing dilute dispersions of poly(methyl methacrylate-block-styrene) (PMMA-*b*-PS) in a matrix of either poly(methyl methacrylate) (PMMA) or poly(vinyl chloride) (PVC) are described. PMMA and PVC species having molecular weights ranging from 25 000 to 400 000 and from 120 000 to 500 000, respectively, were blended with PMMA-*b*-PS copolymers of molecular weight 20 000, 65 000, 283 000, and 680 000 at a composition of 80 : 20 w/w. The PMMA/PMMA-*b*-PS blends exhibit a variety of micellar morphologies (viz. spherical, cylindrical, vesicular, and lamellar structures) which can be systematically modified by varying the molecular weight ratio of homopolymer PMMA to block segment PMMA, $\lambda = M_H/M_A$. For blends in which $\lambda \ll 1$, spherical micelles of uniform size are formed. On increasing λ, the micellar size increases initially, and then a transition from spherical to cylindrical to vesicular and lamellar morphology occurs, provided λ remains less than 1. Further increase of λ to values larger than 1 produces morphologies in which macrophase separation accompanies microphase formation. The PVC/PMMA-*b*-PS blends exhibit microphase formation, even at $\lambda > 1$, due to the strong exothermic interaction between PVC and PMMA. The morphology of this blend system was studied as a function of λ and of the product $N\chi_{PVC\text{-}PS}$, where $\chi_{PVC\text{-}PS}$ is the PVC–PS Flory–Huggins interaction parameter, and $N = N_{PVC}N_{PS}/(N_{PVC}^{\frac{1}{2}} + N_{PS}^{\frac{1}{2}})^2$. Macrophase formation is observed when $\lambda \gg 1$ and also occurs when $\lambda < 1$, if $N\chi_{PVC\text{-}PS}$ becomes very large. Microphase morphology in the PVC/PMMA-*b*-PS blends is insensitive to the value of λ because of the dominant role played by the exothermic interaction in determining coronal swelling of the block copolymer.

(Keywords: block copolymer blends; morphology; effects of molecular weight)

INTRODUCTION

Polymer blends are an attractive route to formation of novel materials whose properties may be a useful combination of those of the blend components. However, most polymers are immiscible and form discrete phases often with high interfacial tension which results in a sharp interface between the two phases and leads to poor mechanical properties of the blend. Addition of a block copolymer improves[1–12] the properties of immiscible polymer blends by decreasing the interfacial tension, resulting in smaller disperse phase sizes, and may also enhance interfacial adhesion between the phases. To be effective, each segment of the block copolymer must have good solubility with one of the blend components. Thus, an understanding of the factors which influence the relative tendency for microphase vs macrophase formation in homopolymer/block copolymer blends is fundamental to optimal application of block copolymers to compatibilize blends of immiscible homopolymers.

Studies of binary blends of a block copolymer with a homopolymer which has the same chemical structure as one block segment (A/A-*b*-B systems) have led to a basic understanding of the factors which influence their phase behaviour[13–30]. The morphological features are dependent on temperature, blend composition, block copolymer structure, and the molecular weight of both block copolymer and homopolymer. Specifically, it is well established[13–30] that the molecular weight ratio between homopolymer and the compatible block segment ($\lambda = M_H/M_A$) is a crucial parameter which determines the degree of solubilization of homopolymer into the block copolymer domain. Thomas and coworkers[26–30] studied blends of polystyrene/poly(styrene-*b*-isoprene) (hPS/PS-*b*-PI) and polystyrene/poly(styrene-*b*-butadiene) (hPS/PS-*b*-PB) in which hPS of molecular weights ranging from 2100 to 36 700, were blended with either PS-*b*-PI or PS-*b*-PB copolymers having molecular weights varying from 20 000 to 160 000. In hPS/PS-*b*-PB blends, where the block copolymer concentration is relatively dilute, it was clearly shown that increase of hPS molecular weight results in a change in micellar morphology: for example, blends of 7 wt% SB 40/40 (molecular weight 87 300) with hPS exhibited[30] a morphological change from spherical ($\lambda = 0.18$ and 0.41) to cylindrical ($\lambda = 0.71$) to lamellar ($\lambda = 0.87$) micelles as the molecular weight of hPS increased. These results indicate that, when $\lambda < 1$, the homopolymer can effectively mix with the compatible block segment. Under these

* To whom correspondence should be addressed

circumstances, the system undergoes microphase separation, the morphology being determined by the degree to which the homopolymer swells the compatible block segment. When $\lambda \gg 1$, the homopolymer cannot effectively solubilize in the compatible block segment, leading to macrophase separation[26–30].

The theoretical criteria for block copolymer micelle formation have been discussed[21–25]. At low volume fraction of block copolymer, Mayes and de la Cruz[25] have discussed theoretically the relative stability of spherical and cylindrical micelles as a function of the molecular weight and concentration of the blend components, and the repulsive Flory–Huggins interaction parameter, χ, between the dissimilar monomers. Expressions for the free energy of cylindrical and spherical structures were proposed and evaluated as a function of concentration and molecular weight[25]. It was concluded that formation of cylindrical micelles is favoured by increasing homopolymer molecular weight and increasing block copolymer volume fraction. The former decreases the entropy of mixing of homopolymer with the micellar corona, therefore more block copolymer chains aggregate into micelles. Similarly, an increase in concentration of block copolymer results in a larger number of block copolymer chains aggregated into micelles. In each case, the cylindrical geometry is favoured due to the ability to accommodate additional chains without significant change in configuration of the block copolymer. These predictions are in qualitative agreement with the experimental observations on micellar morphology by Thomas *et al.*[26–30].

Lowenhaupt and Hellmann[16] have carried out extensive morphological studies of solvent-cast blends containing poly(methyl methacrylate) (PMMA) and poly(methyl methacrylate-block-styrene) (PMMA-*b*-PS), i.e. PMMA/PMMA-*b*-PS systems. The possibility that phase separation in these blends proceeds via either microphase or macrophase separation was theoretically evaluated by mean field calculations and predicted to be dependent on molecular weight of homopolymer and block copolymer and, most importantly, on the chain length ratio (λ) between homopolymer and block copolymer. At room temperature, blends with $\lambda = 2.9$ are predicted to show only macrophase separation, blends with $\lambda = 0.19$ or $\lambda = 0.50$ to show only microphase separation, and blends with $\lambda = 0.87$ or $\lambda = 1.0$ to show macrophase separation if the PMMA homopolymer concentration is high, otherwise microphase separation. In addition, morphological trends observed in blends of PMMA-*b*-PS of molecular weight 175 000 with PMMA homopolymers, having molecular weights 35 000, 95 000, 161 000, 188 000, and 535 000 (corresponding to $\lambda = 0.19$, 0.50, 0.87, 1.0 and 2.9, respectively), at different temperatures and different blend compositions, were in good agreement with the theoretical prediction. In this study[16], only a single molecular weight of block copolymer was used and no analysis was made of any changes in morphology of the microphase as the value of λ was varied.

It has been shown theoretically[31–33] and experimentally[31–38] that a specific interaction between block copolymer and homopolymer, e.g. hydrogen bonding, can be an additional favourable driving force for microphase formation. The favourable enthalpy of mixing obtained from contacts between the homopolymer chains and the compatible block segment compensates for the entropy loss due to the configurational restriction of long-chain homopolymers[31–33]. Therefore, solubilization of homopolymer into the compatible block, and hence microphase formation is obtained despite a high molecular weight ratio. Lowenhaupt *et al.*[37] investigated microphase and macrophase formation in both athermal (A/A-*b*-B) and exothermic (C/A-*b*-B) blends. Theoretical analysis within the mean-field, random phase approximation (RPA) predicts microphase formation dominates in C/A-*b*-B systems even when the molecular weight ratio λ is high enough to cause macrophase separation in A/A-*b*-B blends. Morphological investigations in blends containing a PMMA-*b*-PS block copolymer of molecular weight 175 000 with different homopolymers, viz. poly(styrene-*co*-acrylonitrile) (SAN 215 000), and polycarbonate of bismethyl A (PC 31 000), each of which has exothermic mixing with PMMA, and poly(cyclohexyl methacrylate) (PCHMA 212 000), and tetramethylpolycarbonate (TMPC 183 000), having exothermic interactions with PS were conducted. The results showed that, consistent with the RPA analysis, microphase formation is obtained at molecular weight ratios λ which are high enough to lead to macrophase separation in the corresponding athermal blend PMMA/PMMA-*b*-PS.

However, as pointed out by Adedeji *et al.*[38], the repulsive (endothermic) interaction between the homopolymer and the incompatible block plays an important role in determining the morphology of solvent-cast blends. Moreover, the effect of molecular weight on phase formation and phase morphology in C/A-*b*-B blends has not been extensively explored. Adedeji *et al.*[38] demonstrated in blends of poly(vinyl chloride) (PVC) with poly(*n*-butyl methalcrylate-*b*-styrene) (PnBMA-*b*-PS) that the morphology with respect to microphase- or macrophase formation is influenced by both the exothermic interaction between PVC and PnBMA and the repulsive interaction between PVC and PS. The latter produces a dependence of the morphology on the molecular weights of the PVC, N_{PVC}, and the incompatible PS block, N_{PS}, which can be discussed in terms of the thermodynamic product $N\chi_{PVC\text{-}PS}$ where

$$N = N_{PVC}N_{PS}/(N_{PVC}^{\frac{1}{2}} + N_{PS}^{\frac{1}{2}}) \quad (1)$$

and $\chi_{PVC\text{-}PS}$ is the Flory–Huggins interaction parameter, characterizing the repulsion between PVC and the PS block. When $N\chi_{PVC\text{-}PS}$ is small, the exothermic interaction is significant, and only microphase separation is obtained; when $N\chi_{PVC\text{-}PS}$ is large and dominates over the exothermic interaction, macrophase separation is observed. In other studies, on blends of poly(styrene-*co*-acrylonitrile) with PS-*b*-PMMA, Akiyama and Jamieson[35] demonstrated that the relative strengths of the exothermic and endothermic interactions influence microphase morphology, and Adedeji *et al.* showed[39] that if the repulsive term becomes too small, the exothermic mixing is dominant, and the block copolymer dissolves in the matrix polymer.

In the formation of films by the solvent-casting method, two morphologically-distinct mechanisms have been reported. One involves initial formation of macrophase which may be followed by subsequent microphase separation within the macrodomains as solvent is removed (macrophase-induced microphase separation)[16,40]. A second mechanism involves initial

formation of microphase and then subsequent aggregation of microphase into macrodomains (microphase followed by macrophase formation)[16,40]. Schematic ternary diagrams which illustrate how such morphologies might form during solvent evaporation from a non-selective solvent are shown in *Figures 1a* and *1b*, respectively. The morphology formed is dependent on molecular weight, blend composition, Flory–Huggins interaction parameter (χ), temperature, and rate of solvent evaporation. The first set of these parameters determines the phase diagram of the solvent–polymer mixtures, the last influences the morphology through the kinetics of phase separation.

In the following we describe transmission electron microscopy (TEM) studies of the effect of molecular weight on the microphase and macrophase morphology of PMMA/PMMA-*b*-PS blends and PVC/PMMA-*b*-PS blends, when the block copolymer is relatively dilute. The results for the PMMA/PMMA-*b*-PS system are compared with those obtained by Thomas *et al.*[26–30] for PS-*b*-PB/PS and PS-*b*-PI/PS blends, and those of Lowenhaupt *et al.*[16] on PMMA/PMMA-*b*-PS blends. The molecular weight range of homopolymer (PMMA) used in our study is substantially higher, viz. from 25 000 to 400 000, than that used by Thomas and coworkers[26–30]. Different PMMA-*b*-PS molecular weights, viz. 20 000, 65 000, 283 000, and 680 000 were used to extend the study of Lowenhaupt and Hellmann[16] on the morphological change as a function of the molecular weight ratio, λ. For the PVC/PMMA-*b*-PS blends, the results are compared with those discussed above by Lowenhaupt *et al.*[37] and Adedeji *et al.*[38] for blends with exothermic mixing. By varying the molecular weight of PVC, viz. from 120 000 to 500 000, the effect of molecular weight on phase morphology in PVC/PMMA-*b*-PS blends was investigated, and contrasted with results on PVC/PnBMA-*b*-PS blends reported by Adedeji *et al.*[38]

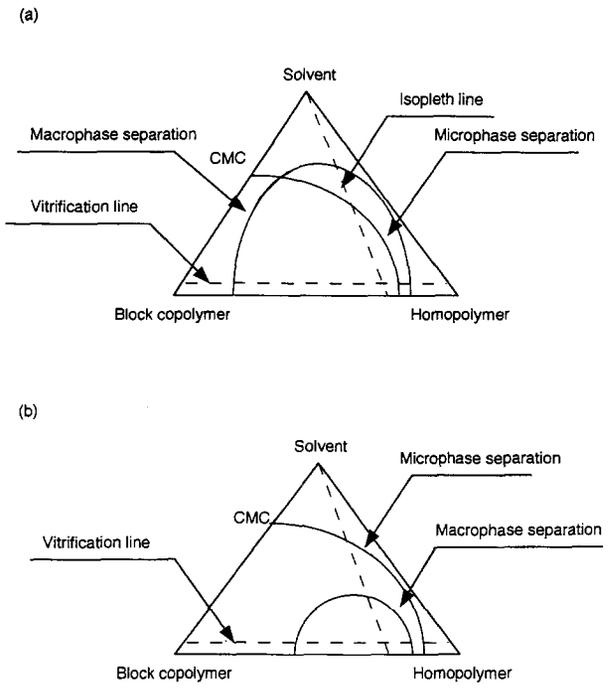

Figure 1 Ternary phase diagram for preparation of phase-separated binary block copolymer/homopolymer blends by evaporation along the isopleth line: two morphological mechanisms are shown: (a) macrophase-induced microphase separation; (b) microphase followed by macrophase separation

EXPERIMENTAL

The materials employed in this study are described in *Table 1*. Stock solutions of each homopolymer (PMMA, PVC), and PMMA-*b*-PS copolymer were prepared in methyl ethyl ketone (MEK) at a concentration 1 g per 100 ml. Binary blends were made by mixing either PMMA or PVC with PMMA-*b*-PS copolymer at a composition ratio 80/20. The molecular weight of the block copolymer was varied (20 000, 65 000, 283 000, and 680 000) together with those of homopolymers, PMMA (25 000, 75 000, 267 000, and 400 000) to make a total of 16 endothermic blend pairs, and PVC (120 000, 175 000, 275 000, and 500 000) to make 16 exothermic blend pairs. The blend films were cast in a narrow glass test tube by slowly evaporating the solvent at room temperature for 3 weeks following which the films were removed and annealed in an oven at 70°C for one day at atmospheric pressure and then under vacuum for one more day to

Table 1 Materials; abbreviations and properties

Abbreviation	$M_W/(\times 10^3)$	M_w/M_n	Copolymer composition[a,b]
PMMA (25 000)[c]	25		
PMMA (75 000)[d]	75		
PMMA (267 000)	267	2.14	
PMMA (400 000)[d]	400	1.43	
PVC (120 000)[d]	120		
PVC (175 000)[d]	175		
PVC (275 000)[d]	275		
PVC (500 000)[e]	500	5.32	
P(MMA-*b*-S) (20 000)[c]	20.5	1.14	10 700/9 800 (0.51)
P(MMA-*b*-S) (65 000)[c]	65.6	1.06	32 500/33 000 (0.53)
P(MMA-*b*-S) (283 000)[f]	283	1.09	163 000/120 000 (0.45)
P(MMA-*b*-S) (680 000)[c]	680	1.10	220 000/460 000 (0.70)

[a] In parentheses we list PS volume fraction of bcp
[b] All bcps show lamellar microphase morphology
[c] Purchased from Polysciences, Inc.
[d] Purchased from Scientific Polymer Products
[e] Purchased from Sigma Chemical Company
[f] Purchased from Polymer Laboratories, Inc.

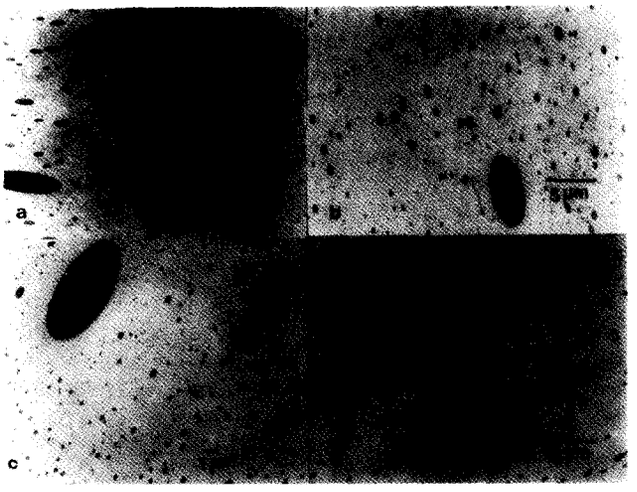

Figure 2 Macrophase separation occurs in PMMA-*b*-PS (20 000)/PMMA blends for PMMA of different molecular weights: (a) 25 000; (b) 75 000; (c) 267 000; (d) 400 000

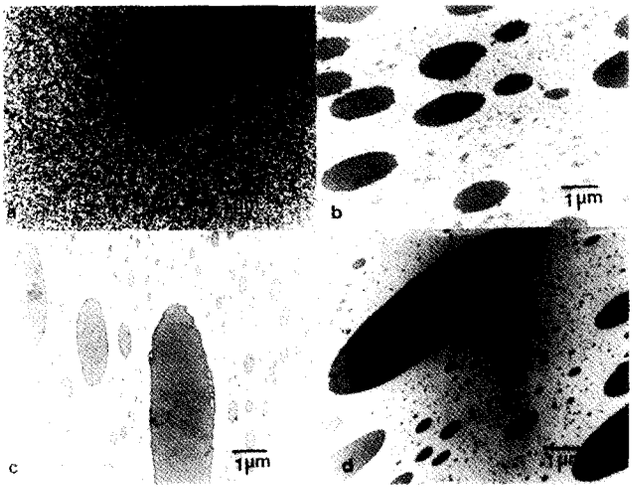

Figure 3 Morphological variation in PMMA-*b*-PS (65 000)/PMMA blends as a function of PMMA molecular weight: (a) PMMA (25 000) shows uniform worm-like micelles; (b) PMMA (75 000) shows aggregation of worm-like micelles; (c) PMMA (267 000) shows macrophase separation; (d) PMMA (400 000) shows macrophase separation

remove all final traces of solvent. The blend films then were sectioned perpendicular to the surface with a thickness of 60 nm using an ultramicrotome (RMC Inc. MT-7000). The thin film sections were picked up on a copper grid to prepare for TEM examination. The specimens were exposed to ruthenium tetroxide (RuO_4) vapour (1.5% aqueous solution) in a closed chamber for 45 min to enhance the contrast in TEM. Polystyrene is stained by RuO_4 and shows dark regions in a bright field image which was viewed with a JEOL JEM-100SX TEM at 100 kV.

RESULTS AND DISCUSSION

First, we point out that the PMMA and PVC homopolymers used in this investigation are polydisperse which means there is a distribution of values of the molecular weight ratio λ. Therefore, we compute an average value of λ from the weight average molecular weight, which we label as λ_w and a corresponding value from the number-average molecular weight, which we label λ_n. Further, we remind the reader that the blend

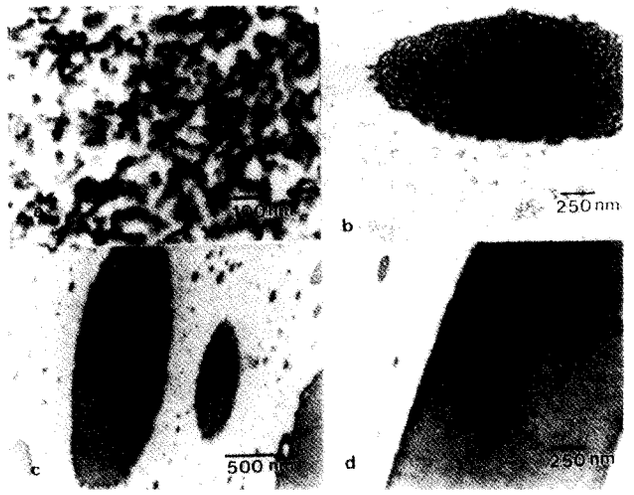

Figure 4 *Figure 3* at high resolution: (a) the wormlike structure of the micelles in PMMA (25 000) is clearly evident; (b) short-range and long-range clustering of worm-like micelles is clearly seen in PMMA (75 000); (c) and (d) the macrodomains enriched in block copolymer in PMMA (267 000) and (400 000) show finely-divided internal microstructure similar to that of the neat block copolymer

films were prepared by solvent-casting from a non-selective solvent (MEK). Thus, initially, the three-component system forms a single phase solution. As solvent is slowly evaporated, the solution composition moves along the isopleth lines in the ternary diagrams (see *Figure 1*), and phase separation takes place in a manner dictated primarily by the net repulsive and attractive interactions of homopolymer and block copolymer. Since the glass transition temperatures of PVC, PS and PMMA are >60°C, upon complete solvent extraction, the residual pseudo-equilibrium morphological structures are permanently fixed at room temperature, and can then be probed by TEM. All TEM micrographs shown are of blends containing PMMA-*b*-PS copolymer and homopolymer at the same blend composition, 80% volume of either PMMA or PVC and 20% volume PMMA-*b*-PS, but differing in the molecular weight of homopolymer and/or block copolymer. Finally, we present data on domain sizes measured from the micrographs, but it should be acknowledged that such values may be influenced by various artifacts such as beam damage-induced dimensional changes, swelling of PS by the RuO_4 stain, grey level subjectivity, and 3D to 2D projection. More accurate microstructure characterization may be possible via small-angle X-ray scattering[41].

PMMA/PMMA-b-PS endothermic blends

Blends containing PMMA-b-PS (20 000). As evident in *Figures 2a–d*, blends containing PMMA-*b*-PS (20 000) show macrophase separation for all PMMA homopolymer molecular weights, corresponding to molecular weight ratios $\lambda_w = 2.34$, 7.0, 24.95, and 37.38. Here the PMMA segment is too small to solubilize PMMA homopolymer, and therefore, the blend exhibits macrophase separation to form discrete block copolymer-rich macrodomains separated from the PMMA-rich domain. No microstructure is evident within these macrodomains. From the work of Amundson *et al.*[42], we estimate the ODT temperature of PMMA-*b*-PS (20 000) to be 117.5°C, i.e. comparable to the glass

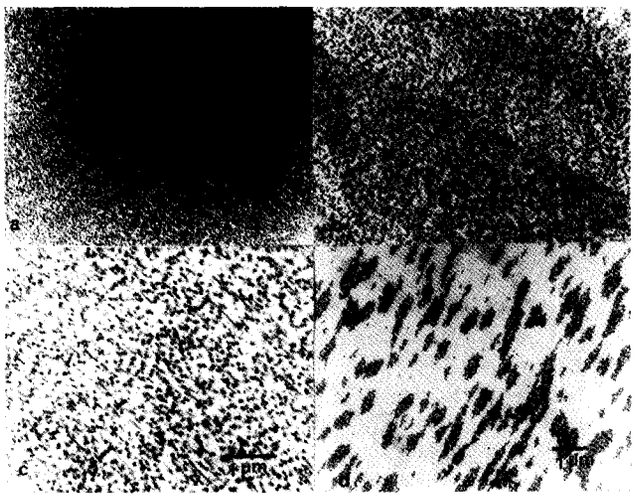

Figure 5 Morphology of PMMA (283 000)/PMMA blends as a function of PMMA molecular weight: (a) uniformly-dispersed spherical micelles in PMMA (25 000); (b) uniformly-dispersed spherical micelles in PMMA (75 000); (c) cylindrical micelles in PMMA (267 000); (d) aggregation of cylindrical micelles in PMMA (400 000)

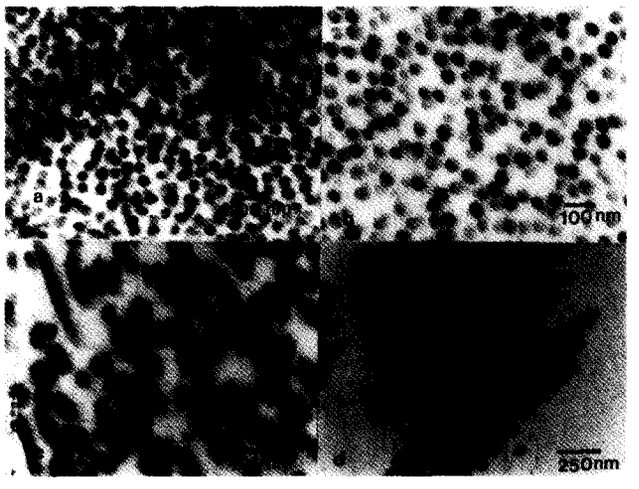

Figure 6 *Figure 5* at high resolution: (a) and (b) the spherical micellar structure in PMMA (25 000) and (75 000) is clearly seen; micelles which are fully enclosed in the thin section show the darkest stain; (c) and (d) the wormlike structure of the micelles in PMMA (267 000) and (400 000) is clearly seen

transition temperatures (T_g) of PMMA and PS which are 105 and 100°C, respectively. Therefore, it is possible that, during solvent evaporation and following macrophase separation, the T_g within the block copolymer-rich macrodomains becomes essentially the same as the ambient temperature, and hence the blend morphology is fixed before the order–disorder transition can occur. Also it is interesting that the shapes of the macrodomains are ellipsoidal. The origin of this effect is unknown, and may reflect the development of internal stresses or gravitational settling during drying of the films.

Blends containing PMMA-b-*PS (65 000).* In the blends containing PMMA-*b*-PS (65 000), the morphological results indicate a trend from microphase toward macrophase separation on increasing the molecular weight ratio λ, as shown in *Figures 3a–3d*, and at higher resolution in *Figures 4a–4d*. With PMMA (25 000) (*Figures 3a* and *4a*), a uniform dispersion of worm-like micelles is found, which indicates effective solubilization of PMMA in the micellar corona. This is consistent with the fact that the molecular weight ratio $\lambda < 1$ ($\lambda_w = 0.77$). The worm-like micelles have an average width of 31.25 nm and an average length of 125 nm. The degree of solubilization is high enough for microphase to form but not so high to produce spherical micelles. At higher homopolymer molecular weight, PMMA (75 000) as shown in *Figure 3b* and at high resolution in *Figure 4b*, worm-like micellar structures are observed, similar to those seen with PMMA (25 000). However, these micelles apparently self-associate into macrodomains about 2 μm in size which coexist with free worm-like micelles. The evidence that free worm-like microstructures are present, as well as a variety of intermediate states of aggregation, in the PMMA matrix outside the macrodomains, suggests that microphase separation occurs initially and subsequently the system undergoes macrophase separation via aggregation of the microstructures, i.e. microphase followed by macrophase separation, as previously reported in PMMA/PMMA-*b*-PS blends by Lowenhaupt and Hellmann[16]. The degree to which PMMA (75 000) can wet the block copolymer corona is limited since the molecular weight ratio, $\lambda_w = 2.3$, is substantially larger than unity. Thus, as solvent evaporates, the system attempts to reduce the contact area between PMMA block segments and PMMA homopolymer chains by aggregation of the micelles. It is interesting that in *Figures 3b* and *4b*, one sees a high concentration of PMMA (75 000) in the area immediately surrounding the macrodomains which may reflect the rejection of PMMA homopolymer from the block copolymer-rich domains.

As the PMMA molecular weight is increased further to 267 000 and 400 000, we find macrodomains which exhibit some internal microstructure, dispersed in a matrix of PMMA homopolymer as shown in *Figures 3c* and *3d*, respectively. The size of the macrodomains varies from 0.5 to 7.0 μm. Very few freely-dispersed microstructures appear. The intra-domain structure appears to be more finely divided in the blend containing PMMA (400 000). It appears likely that a similar mechanism, viz. microphase followed by macrophase separation, operates in these two blend systems. Thermodynamic considerations suggest, however, that as the molecular weight of PMMA homopolymer increases, the block copolymer-rich phase will become more depleted in homopolymer. Thus, as the solvent evaporates and the system undergoes micellar aggregation, more of the high molecular weight PMMA chains are rejected from the macrodomains. Hence, in *Figures 3b–3d* it is evident that the PMMA content of the macrodomains progressively decreases.

Blends containing PMMA-b-*PS 283 000.* The morphology of the blends containing block copolymer PMMA-*b*-PS (283 000) shows a striking systematic variation as the molecular weight ratio λ_w increases, shown in *Figures 5a–5d* and at high resolution in *Figures 6a–6d*. The blend with PMMA (25 000) ($\lambda_w = 0.15$) exhibits monodisperse spherical micelles of diameter 34.5 nm (*Figures 5a* and *6a*). Contrasting this with the PMMA (25 000)/B(65 000) blend ($\lambda_w = 0.77$), which shows worm-like micelles (*Figures 3a* and *4a*), we see that the spherical morphology reflects the higher solubility of the 25 000 homopolymer in the PMMA segment of the B (283 000) copolymer. For reference, we estimate

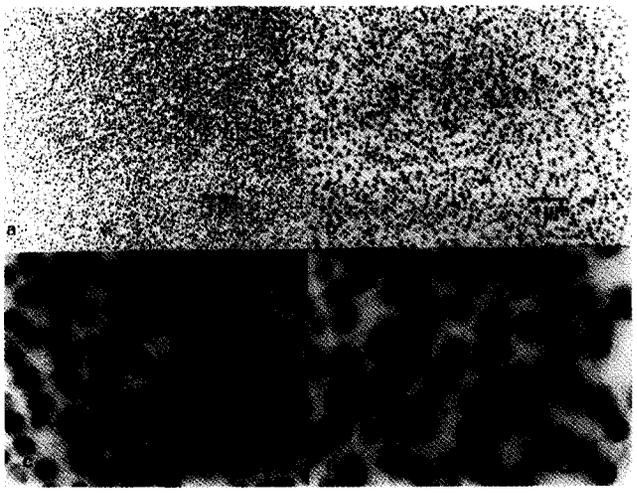

Figure 7 Morphology of PMMA-*b*-PS (680 000) PMMA blends with different PMMA molecular weights: (a) spherical micelles in PMMA (25 000); (b) spherical micelles of larger size in PMMA (75 000); (c) spherical micelles in PMMA (25 000) at high resolution; (d) spherical micelles in PMMA (75 000) at high resolution

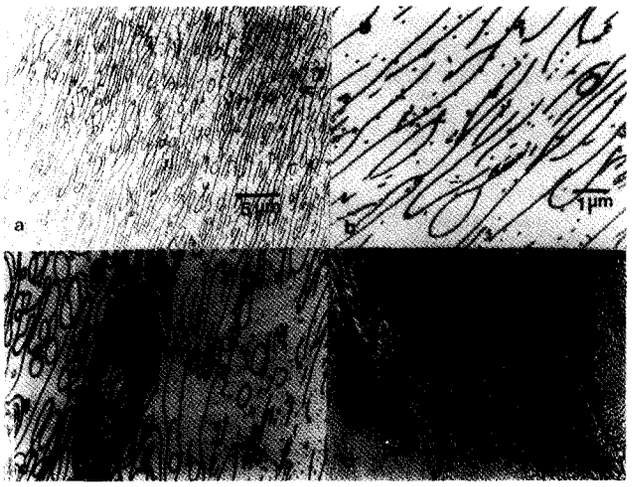

Figure 8 Morphology of PMMA-*b*-PS (680 000)/PMMA (267 000) blend probed in different regions of the film: (a) and (b) regions of high PMMA concentration; (c) region of intermediate PMMA concentrations; (d) region of low PMMA concentration

the root-mean square end-to-end distance of the PS segment in the PMMA-*b*-PS (283 000) copolymer to be 23.4 nm, assuming a Gaussian chain[42,43]. In the blend containing PMMA (75 000), *Figures 5b* and *6b*, we again find a monodisperse spherical microdomain morphology. However, the micelles are larger in size, having a diameter of 40.6 nm, and the average intermicellar separation distance is also larger. In this system, the molecular weight ratio ($\lambda_w = 0.46$) is still small enough that the homopolymer chains can very effectively solubilize into the PMMA block segments, causing strong expansion of the PMMA block. However, the degree of swelling and, hence, the interfacial curvature is not so high as in the PMMA 25 000/B 283 000 blend. The polystyrene chains in the core of the micelles are therefore not so compressed and a larger number of block copolymer chains can be accommodated into a single spherical micelle.

Further increase of the molecular weight of PMMA homopolymer to 267 000 results in a morphological change to cylindrical micelles (*Figure 5c*) with an average diameter of 43.75 nm and an average length of 250 nm. This is consistent with the expectation that the 267 000 PMMA exhibits a further decrease in solubility in the PMMA micellar corona, and hence there is a further reduction in corona swelling and less contraction of the polystyrene core. Thus more block copolymer chains aggregate into micelles, and the spherical structure, observed in PMMA (75 000), transforms, in PMMA (267 000), to a cylindrical microstructure consistent with the theoretical discussion by Mayes *et al.*[25]. Further increase in the molecular weight of PMMA homopolymer to 400 000 produces a morphology where the cylindrical micelles become aggregated into macrodomains in a matrix of essentially pure PMMA homopolymer (*Figures 5d* and *6d*). Thus the morphology of the PMMA (400 000)/PMMA-*b*-PS (283 000) blend appears rather similar to that of the PMMA 75 000/PMMA-*b*-PS (65 000) system (*Figure 3b*). In this regard, it is interesting to note that the molecular weight ratios of each blend are similar ($\lambda_w = 2.31$ for the former, $\lambda_w = 2.45$ for the latter).

Blends containing PMMA-b-*PS (680 000).* Morphologies of the blends containing PMMA-*b*-PS (molecular weight 680 000) with the various PMMA homopolymers are shown in *Figures 7* to *9a–d*. The blend with PMMA (25 000) has a very low molecular weight ratio ($\lambda_w = 0.11$), resulting in a morphology of uniformly-distributed spherical domains of narrow size distributed with average diameter of 75 nm (*Figures 7a* and *7c*). For reference, the unperturbed root-mean square end-to-end distance of polystyrene[43] in PMMA-*b*-PS copolymer (680 000) is estimated to be 46 nm. The blend with PMMA (75 000) also shows uniformly distributed spherical micelles which, however, are polydisperse in size with an average domain diameter of 93.75 nm (*Figures 7b* and *7d*). The increase in size and in the average intermicellar separation distance compared to the blend with PMMA (25 000) is due to the same effect discussed above for PMMA-*b*-PS (283 000) viz. a decrease in swelling of the micellar corona results in a reduction in compression of the micellar core, and hence an increase in micellar aggregation number.

The PMMA-*b*-PS (680 000)/PMMA (267 000) blend shows a more complex morphology (*Figures 8a–8d*). Here macrophase separation occurs as evidenced by visual examination of the films which show turbid regions and transparent regions. Examination of the transparent parts of the film, representing regions of high concentration of PMMA homopolymer, shows microdomain morphology consisting of uniformly-distributed vesicular, and cylindrical and perhaps sheet-like structures (*Figures 8a* and *8b*). The evidence for vesicular and cylindrical microstructures is very clear. Different perspectives of the cylindrical micelles are apparent in these micrographs which result from different orientations of the cylinder axis to the direction of sectioning. For example, if the micellar axis is perpendicular to the section surface, one sees the spherical cross section. Alternatively, if the cyclinder is aligned at an angle to the section surface, it is seen as an elongated structure, the length increasing as the angle decreases. Evidence for sheet-like microstructures is not so definitive but it seems very likely that the ubiquitous exceedingly-long threadlike objects represent sections through sheet-like micelles, rather than longitudinal sections

through cylindrical micelles. Lamellar aggregates are not found because of the low concentration of block copolymer in this region. Interestingly, it is evident that the sheet-like micelles appear to show a high degree of parallel orientation. The reason for this is unknown, but must reflect non-equilibrium processes occurring during film drying. The morphology in the turbid areas of the film, where there is a low concentration of PMMA homopolymer, shows macrodomains with loosely-ordered lamellae and cylinders. These coexist with disordered lamellae and cylinders, reflecting local variations in solubilization of homopolymer in the PMMA segments of the block copolymer (*Figure 8d*). Inspection of other parts of the film shows a transitional morphology where the microstructure varies from lamellar to isolated sheets, cylinders, and vesicles depending on the local concentration of PMMA homopolymer (*Figure 8c*).

Because of the high molecular weight ratio ($\lambda_w = 1.21$), there is limited coronal solubility of the PMMA (267 000), and therefore only cylindrical, sheet-like and vesicular structures are observed. The observation that long-range fluctuations in concentration of homopolymer and block copolymer occurs is a strong indication that macrophase separation has occurred initially during the solvent evaporation process, followed by microphase separation[40]. This reflects an increase in the repulsion between the homopolymer PMMA and the PS block segment of the block copolymers, i.e. the product $N\chi_{PS/PMMA}$ becomes sufficiently large to induce macrophase separation.

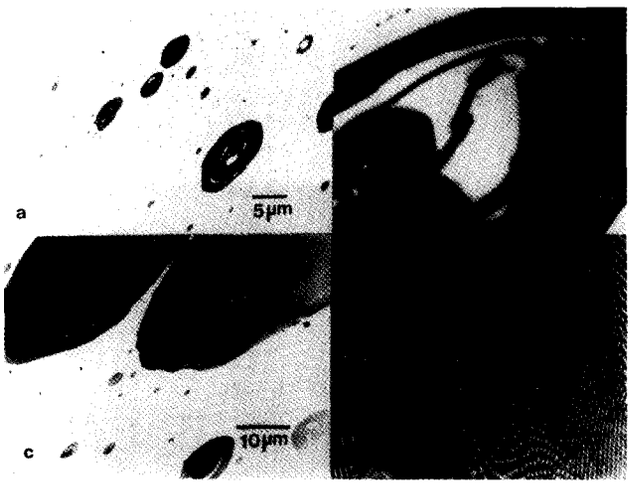

Figure 9 Morphology of PMMA-*b*-PS (680 000)/PMMA (400 000) blend probed in different regions of the film: (a) and (b) regions of high PMMA concentration; (c) region of intermediate PMMA concentration; (d) region of low PMMA concentration.

Here $\chi_{PS/PMMA}$ is the pertinent Flory interaction parameter and N is a quantity which depends on the molecular weight of homopolymer PMMA, N_{PMMA}, and PS block segment, N_{PS}:

$$N = N_{PMMA}N_{PS}/(N_{PMMA}^{\frac{1}{2}} + N_{PS}^{\frac{1}{2}}) \quad (2)$$

A similar effect can be observed in the blend of PMMA-*b*-PS (680 000) with PMMA of molecular weight 400 000 again evidenced by macroscopic concentration fluctuations of the blend components (*Figures 9a–9d*). In the turbid block copolymer-rich region, we find an ordered morphology, consisting of cylinders of PMMA in a matrix of PS, as seen in *Figure 9d*. However, the diameter of the PMMA cylinders is reduced since the dissolution of PMMA (400 000) homopolymer in the PMMA corona is less compared to that of PMMA (267 000) as evident by comparing *Figures 9d* and *8d*. This is expected since the molecular weight ratio $\lambda_w = 1.82$ is larger. In areas where the concentration of PMMA is higher, one observes isolated large macrodomains whose interior structure is lamellar (*Figure 9c*). The interior lamellae show some degree of swelling which appears to be higher than in the block copolymer-rich region, presumably indicating these areas are enriched in lower molecular weight PMMA. In areas with a very high concentration of PMMA (*Figures 9a* and *9b*) in the interior structures of some macrodomains of small size, worm-like interior microstructures are found, which may again result from a local excess of low molecular weight PMMA homopolymer.

From the experimental data which is summarized in *Table 2*, disordered spherical micelles are obtained when $\lambda_w < 0.5$, disordered cylinders are obtained when $0.7 < \lambda_w < 1.64$ (worm-like structures which are short cylinders are obtained when $\lambda_w = 0.77$, long cylinders are obtained when $\lambda_w = 1.21-1.64$), microphase followed by macrophase separation is obtained when $2.31 < \lambda_w < 12.31$. Macrodomains are obtained in blends containing low molecular weight block copolymer PMMA-*b*-PS (20 000) ($2.3 < \lambda_w < 37.38$). Comparing our results to the microstructures observed by Thomas *et al.*[26,30], we find that the trends of morphological change with variation in the value of λ are in good agreement. From Winey *et al.*[30], blends of PS-*b*-PB of molecular weight 87 300 with hPS of different molecular weight at a dilute concentration of PS-*b*-PB copolymer (93 vol% of hPS), show disordered spheres obtained at $\lambda = 0.18$, disordered cylinders at $\lambda = 0.71$ and lamellae at $\lambda = 0.87$. The first two are consistent with our observation, but we see lamellae in our system at $\lambda_w = 1.2$ (PMMA-*b*-PS (680 000)/PMMA (267 000)). Note, however, that the PMMA homopolymers used in our study are polydisperse, and that the number-average

Table 2 Molecular weight ratio (λ) between PMMA homopolymer and PMMA block segment

	PMMA-*b*-PS (20 K)			PMMA-*b*-PS (65 K)			PMMA-*b*-PS (283 K)			PMMA-*b*-PS (680 K)		
PMMA	λ_w	λ_n		λ_w	λ_n		λ_w	λ_n		λ_w	λ_n	
25 K	2.34	–	macro	0.77	–	worm	0.15	–	sphere	0.11	–	sphere
75 K	7.0	–	macro	2.31	–	worm aggre	0.46	–	sphere	0.34	–	sphere
267 K	24.95	11.65	macro	8.21	3.84	worm aggre	1.64	0.76	disorder cylinder	1.21	0.57	cylin/vesicle/macro
400 K	37.38	26.14	macro	12.31	8.61	worm aggre	2.45	1.72	cylinder aggre	1.82	1.27	macro

Macro, macrodomains; worm, worm-like microstructures; worm aggre, aggregation of worm-like microstructures; sphere, spherical micelles; cylinder aggre, aggregation of cylindrical micelles; cylin, cylinders

Table 3 Molecular weight ratio (λ) and magnitude of repulsion between PVC and PS block segment ($N\chi_{PVC\text{-}PS}$)

	PMMA-*b*-PS (20 000)				PMMA-*b*-PS (65 000)				PMMA-*b*-PS (283 000)				PMMA-*b*-PS (680 000)			
	λ	$N\chi_{PVC\text{-}PS}$	Micro	Macro	λ	$N\chi_{PVC\text{-}PS}$	Micro	Macro	λ	$N\chi_{PVC\text{-}PS}$	Micro	Macro	λ	$N\chi_{PVC\text{-}PS}$	Micro	Macro
PVC																
120 000	11.21	6.3		X	3.7	15.9	X		0.74	36.3	X		0.55	69.2	X	
175 000	16.36	6.7		X	5.38	17.6	X		1.07	42.4		X	0.79	86.1		X
275 000	25.7	7.1		X	8.46	19.5	X		1.68	50.0		X	1.25	109.4		X
500 K	46.7	7.6		X	15.4	21.9	X		3.07	60.1		X	2.27	144.3		X

Note[25]: $N = N_{PVC}N_{PS}/(N_{PVC}^{\frac{1}{2}} + N_{PS}^{\frac{1}{2}})^2$ and $\chi_{PVC\text{-}PS} = 0.992$

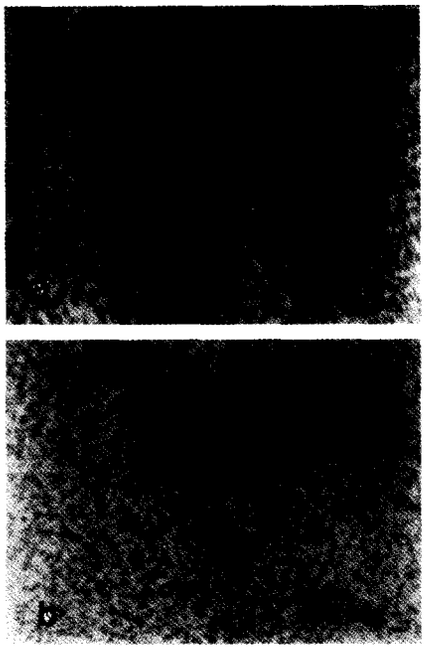

Figure 10 Uniform microphase separation is observed in PMMA-*b*-PS (65 000)/PVC blends for PVC of different molecular weight: (a) PVC (120 000); (b) PVC (500 000)

value of λ in this system is $\lambda_n = 0.57$, suggesting that in polydisperse systems, it may be λ_n which determines the phase separation behaviour.

PVC/PMMA-b-*PS exothermic blends*

Blends containing PMMA-b-*PS (20 000).* Blends of PMMA-*b*-PS 20 000 with PVC of molecular weights 120 000, 175 000, 275 000, and 500 000, all show macrophase separation manifested as discrete macrodomains of PMMA-*b*-PS in a matrix of PVC homopolymer. The macrodomains show no internal microstructure, for which we suggest the same explanation offered with regard to PMMA/PMMA-*b*-PS (20 000) blends. Considering the very large values of the molecular weight ratio between PVC and the PMMA block listed in *Table 3* ($\lambda_w = 11.21$, 16.36, 25.7, and 46.7 for PVC (120 000), (175 000), (275 000), and (500 000), respectively), and the small values of the product $N\chi_{PVC\text{-}PS}$ for these blends, we deduce that a low entropy of mixing plays the dominant role in producing macrophase separation. Evidently, the PVC chains are too large, relative to the small PMMA block segment (only 10 700), the exothermic interaction cannot compensate for the small entropy of mixing, and the system undergoes macrophase separation.

Blends containing PMMA-b-*PS (65 000).* Blends of PMMA-*b*-PS 65 000 with PVC of molecular weight 120 000, 175 000, 275 000, and 500 000 all show uniformly dispersed microphase separation as illustrated in *Figures 10a* and *10b* for blends of PMMA-*b*-PS (65 000) with PVC (120 000) and PVC (500 000). From *Table 3*, the molecular weight ratio, λ, in these blends is much larger than unity ($\lambda_w = 3.7$, 5.4, 8.5, and 15.4 for PVC (120 000), (175 000), (275 000), and (500 000), respectively). The evidence of microphase separation

Figure 11 Morphology of PMMA-*b*-PS (283 000)/PVC blends for PVC of different molecular weights: (a) PVC (120 000) shows uniform microphase separation; (b) PVC (178 000), (c) PVC (275 000), and (d) PVC (500 000) each show long-range spatial fluctuation in concentration of microstructures

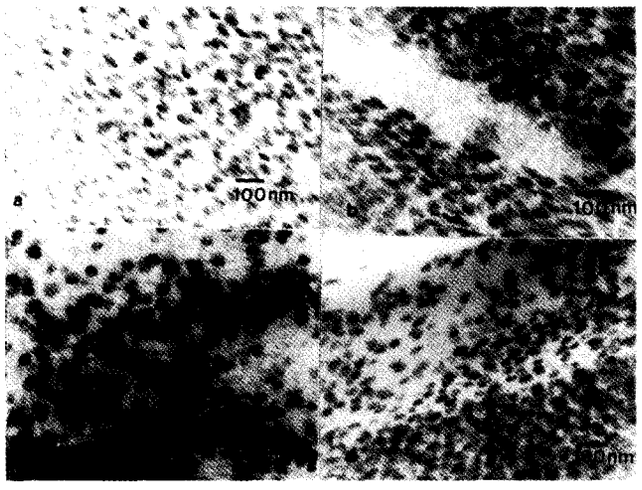

Figure 12 *Figure 11* at high resolution: the ellipsoidal shapes of the micelles formed in these blends is clearly evident when sectioned through their major axis

with no hint of macrophase separation in the blend of PMMA-*b*-PS (65 000) with PVC (500 000) (*Figure 10b*) where the molecular weight ratio is very high ($\lambda = 15.4$), clearly demonstrates the dominant role is played by the strong exothermic interaction between PVC and PMMA ($\chi_{PVC\text{-}PMMA}$). The respective values of $N\chi_{PVC\text{-}PS}$, viz. 15.9, 17.6, 19.5, and 21.9 (*Table 3*), are evidently not high enough to induce macrophase separation during the solvent-casting process. In contrast to the morphology of PMMA/PMMA-*b*-PS (65 000) blends which show (*Figure 3*) worm-like microstructure (PMMA 25 000), and aggregation of worm-like structures into macrodomains (PMMA 75 000, 267 000, and 400 000), the PVC blend system shows elliptical micelles. The average size of the micelles in both PVC (120 000) and PVC (500 000) is 31.3 nm along the major axis and 13 nm along the minor axis. This clearly indicates more effective solubilization of PVC in the PMMA segment, even when the molecular weight of the PVC is much higher than that of the PMMA segment. The origin of the ellipsoidal shape of the microstructure in this PVC blends is not yet understood. A similar characteristic was also observed in blends of PVC/PnBMA-*b*-PS[38]. The effect is not related to the direction of sectioning, but may reflect the development of internal stresses in the glassy films.

Blends containing PMMA-b-*PS (283 000).* When the molecular weight of PMMA-*b*-PS copolymer increases to 283 000, the exothermic interaction still enhances solubilization of PVC in the PMMA block, as seen by the formation of elliptical microstructures even at high molecular weight ratio in PVC (500 000) ($\lambda = 3.07$). However, uniformly-dispersed microstructures are obtained only for PVC (120 000) where $N\chi_{PVC\text{-}PS}$ is 36.3. Due to the different shapes of the micelles in the PVC and PMMA blend systems, we compare the micellar structures in terms of the micellar volumes. We find that the volume of the elliptical micelles in the PVC (120 000)/PMMA-*b*-PS (283 000) blend is comparable to that of the spherical micelles in the PMMA (25 000)/PMMA-*b*-PS (283 000) blend, which suggests that PVC (120 000) solubilizes into the PMMA block segment to a degree comparable to that of PMMA (25 000) again reflecting the exothermic mixing of PVC and PMMA. As the molecular weight of PVC increases to (175 000), there appear long-range fluctuations in concentration of the microstructures in the form of discrete PVC rich regions (*Figures 11b* and *12b*). This suggests that, despite a relatively low molecular weight ratio ($\lambda = 1.07$), as solvent is evaporated, macrophase separation occurs first and then the system undergoes microphase separation due to the strong repulsion between the high molecular weight PVC and the PS block ($N\chi_{PVC\text{-}PS} = 42.4$). Further increase in the repulsive interaction by increasing the molecular weight of PVC to 275 000 and 500 000, corresponding to $N\chi_{PVC\text{-}PS} = 50.0$ and 60.1, respectively, produces an increase in the volume fraction of the PVC-rich macrodomains (*Figures 11c* and *12c*, and *11d* and *12d*).

A distinctive feature of our observations, in both the PVC/PMMA-*b*-PS (65 000) and PVC/PMMA-*b*-PS (283 000) blend systems, is that, in contrast to our results in the PMMA/PMMA-*b*-PS blends, we see no evidence of a transition to wormlike micelles, or, indeed, little change in micellar size, as the matrix molecular weight is increased. Notwithstanding the uncertainty introduced by the unknown polydispersities of the PVC samples, it seems clear that a major contributor to this effect is the dominant role played by the exothermic interaction in controlling the coronal swelling of the micelles. To illustrate this, we utilize an expression[44,45] for the thickness, L, of a polymer brush of molecular weight N, attached to an impenetrable wall, in contact with a polymer matrix of molecular weight, P, with which it has an exothermic interaction, characterized by a negative Flory interaction parameter, χ:

$$(L/L_{ref})^3 = (N/P) - 2N\chi \qquad (3)$$

where L_{ref} is the brush length of the neat block copolymer. For purposes of discussion, we may equate P/N to the values of the molecular weight ratio λ specified for these two blends in *Table 3* where we find that λ varies from 0.74 to 15.4, corresponding to a variation in N/P from 1.35 to 0.065. From equation (3), it follows that, if the term $-2N\chi$ is much larger than

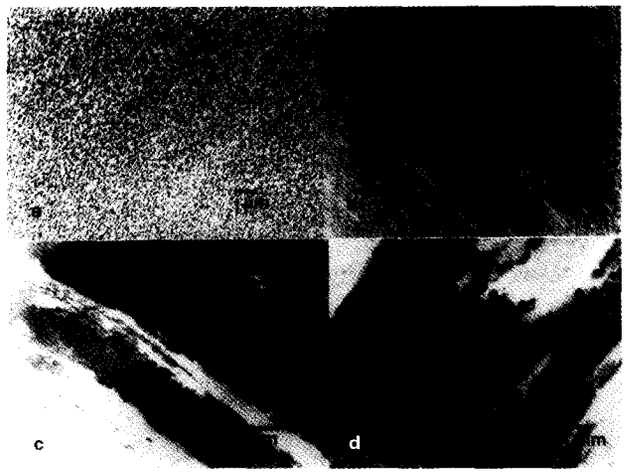

Figure 13 Morphology of PMMA-*b*-PS (680 000)/PVC blends for PVC of different molecular weights: (a) PVC (120 000) shows uniform microphase separation; (b) PVC (175 000) shows long-range spatial fluctuation in concentration of the microstructures; (c) PVC (275 000) and (d) PVC (500 000) show macrophase-induced microphase separation

1.35, the effect of molecular weight is diminished. Noting that an experimental study[46] indicates $\chi_{PVC/PMMA} = -0.257$, such an interpretation appears reasonable in the PVC/PS-*b*-PMMA system.

Blends containing PMMA-b-*PS (680 000).* For blends containing PMMA-*b*-PS copolymer (680 000), only that with PVC (120 000) shows uniformly-dispersed micelles (*Figure 13a*). Here both the exothermic interaction and the entropy of coronal mixing are favourable ($\lambda = 0.55$). Because the $N\chi_{PVC\text{-}PS}$ value in this blend is 69.2 which is slightly higher than that of PVC (500 000)/PMMA-*b*-PS (283 000) ($N\chi_{PVC\text{-}PS} = 60.1$), the system might be expected to undergo macrophase separation because the exothermic driving force is overcome by the repulsive interaction. Since, however, the blend shows uniform microphase separation, we infer that the entropic contribution from coronal mixing tips the balance in favour of microphase formation. Note that the molecular weight ratio $\lambda = 0.55$ is much smaller than that of the PVC (500 000)/PMMA-*b*-PS (283 000) blend ($\lambda = 3.07$). Increase of molecular weight of PVC to 175 000 results in an increase of $N\chi_{PVC\text{-}PS}$ to 86.1, which is apparently too large to be compensated for by the entropic contribution from coronal mixing ($\lambda = 0.79$), as evidenced by the appearance (*Figure 13b*) of long-range spatial fluctuations in the concentration of micelles, i.e. formation of PVC-rich regions. It should be mentioned that in this system, the effect of exothermic interaction in promoting interfacial solubilization of PVC in the PMMA corona is still evident in that microphase separation leads to small elliptical micelles. The effect of the repulsive interaction becomes more dramatic as the molecular weight of PVC is increased further to 275 000 and 500 000 where now we observe isolated macrodomains of block copolymer in a matrix of PVC homopolymer (*Figures 13c* and *13d*). The lamellar microstructure observed within these macrodomains indicates essentially complete rejection of the high molecular weight PVC from the PMMA corona, despite the exothermic interaction, due to the very large values of $N\chi_{PVC\text{-}PS}$ (109.4 and 144.3 for PVC (275 000) and (500 000), respectively), coupled with values of λ larger than unity ($\lambda_w = 1.25$ and 2.27, respectively). Of course, because of the extreme polydispersity of the PVC samples, it is likely that some low molar mass PVC is solubilized in the PMMA microdomains.

The morphological behaviour of all PVC blends is summarized in *Table 3* where the propensity for microphase- or macrophase formation, as well as $N\chi_{PVC\text{-}PS}$ value, are listed. PVC/PMMA-*b*-PS blends exhibit microphase separation even at a high molecular weight ratio ($M_H/M_A > 1$) due to the exothermic interaction between PMMA and PVC. This observation is consistent with those reported by Lowenhaupt *et al.*[37] in binary blends of PCHMA, TMPC, and SAN, each blended with PMMA-*b*-PS copolymer which exhibit microphase formation at molecular weight ratio higher than 1, and with the accompanying theoretical calculation. The experimental data reported by these authors, however, covers a relatively limited range of the molecular weight ratio (λ) up to 2.4 (PCHMA/PMMA-*b*-PS blend). In our study, varying the molecular weight of both homopolymer and block copolymer, we explore the morphological behaviour over a much wider range of λ and $N\chi_{PVC\text{-}PS}$ values.

From *Table 3*, PVC/PMMA-*b*-PS blends exhibit microphase separation at $15.9 < N\chi_{PVC\text{-}PS} < 36.3$ and macrophase separation is obtained at $N\chi_{PVC\text{-}PS} > 42.4$. These results show a similar trend to those observed by Adedeji *et al.*[38] in PVC/PnBMA-*b*-PS blends where microphase separation was obtained in the range $22 < N\chi_{PVC\text{-}PS} < 39$ and macrophase separation was obtained at $N\chi_{PVC\text{-}PS} > 39$. Blends which have small $N\chi_{PVC\text{-}PS}$ may exhibit macrophase separation if the ratio $\lambda > 1$, and blends with larger $N\chi_{PVC\text{-}PS}$ may exhibit macrophase separation, even though $\lambda < 1$. In addition, when microphase occurs, we find, again consistent with observations of Adedeji *et al.*[38] for PVC/PnBMA-*b*-PS blends, that, in comparison to endothermic blends, the micellar sizes are smaller, and the shape of the microphase is relatively insensitive to the value of λ, because of the dominant role of the exothermic interaction. It is pertinent to note here, however, that it was earlier shown[35] in binary blends of poly (styrene-*co*-acrylonitrile) (SAN) with PMMA-*b*-PS that a transition from spherical to wormlike micelles can be produced by systematically decreasing the strength of the exothermic interaction between SAN and PMMA, and keeping λ approximately constant. A final caveat in this regard is that, in the PVC (120 000)/PMMA-*b*-PS (65 000) blend, at a composition of 40/60, wormlike micelles are observed[45], suggesting that, in exothermic blends, as for endothermic blends[25,26–30], wormlike micelles are favoured at sufficiently high block copolymer concentration.

CONCLUSIONS

Morphological features in binary PMMA/PMMA-*b*-PS and PVC/PMMA-*b*-PS blends, where the block copolymer concentration is dilute, were investigated. In PMMA/PMMA-*b*-PS blends, systematic effects of molecular weight on the formation of microphase *versus* macrophase and also on the morphology of the microstructures produced were revealed. Our results show a trend from spherical to cylindrical to vesicular or lamellar microstructures, and finally to macrophase separation, with increase of λ, the molecular weight

ratio between homopolymer and the compatible block segment, similar to the observations of Thomas and coworkers[26–30] on blends of PS/PS-*b*-PB and PS/PS-*b*-PI. In PVC/PMMA-*b*-PS blends, it was shown that the exothermic interaction between PVC and PMMA block segment can enhance the tendency for microphase separation in comparison to the endothermic PMMA/PMMA-*b*-PS system, since microphase is formed when $\lambda > 1$, the microdomains are smaller in size and their shapes less sensitive to the value of λ. However, uniform microphase formation is obtained within a window. One limit occurs on increasing molecular weight, due to a too-high repulsion between homopolymer and the incompatible block which leads to macrophase separation. On the other hand, at low molecular weight, macrophase may be formed if the entropy of coronal mixing is too low, due to a very high value of λ.

ACKNOWLEDGEMENTS

We are grateful to the National Science Foundation for financial support of this research through Materials Research Group award DMR 01845. We are also grateful to Professor Steven D. Hudson for useful comments.

REFERENCES

1 Inoue, T., Soen, T., Hashimoto, T. and Kawai, H. *Macromolecules* 1970, **3**, 87
2 Fayt, R., Jerome, R. and Teyssie, Ph. *Makromol. Chem.* 1986, **187**, 837
3 Fayt, R., Jerome, R. and Teyssie, Ph. *J. Polym. Sci., Polym. Lett. Edn.* 1986, **24**, 25
4 Fayt, R., Jerome, R. and Teyssie, Ph. *J. Polym. Sci., Polym. Chem. Edn.* 1989, **27**, 2823
5 Knaub, P., Camberlin, Y. and Gerard, J. F. *Polymer* 1988, **29**, 1365
6 Anastasiadis, S. H., Gancarz, I. and Koberstein, J. T. *Macromolecules* 1989, **22**, 1449
7 Brown, H. R. *Macromolecules* 1989, **22**, 2859
8 Russell, T. P. and Menell, A. *Macromolecules* 1991, **24**, 5721
9 Russell, T. P., Anastasiadis, S. H., Menelle, A. M., Felcher, G. P. and Satija, S. K. *Macromolecules* 1991, **24**, 1575
10 Thomas, S. and Prudhomme, R. E. *Polymer* 1992, **33**, 4260
11 Adedeji, A. and Jamieson, A. M. *Polymer* 1993, **34**, 5038
12 Hu, W., Koberstein, J. T., Lingelser, J. P. and Gallot, Y. *Macromolecules* 1995, **28**, 5209
13 Hashimoto, T., Tanaka, H. and Hasegawa, H. *Macromolecules* 1990, **23**, 4378
14 Koizumi, S., Hasegawa, H. and Hashimoto, T. *Makromol. Chem. Macromol. Symp.* 1992, **62**, 75
15 Winey, K. I., Thomas, E. L. and Fetters, L. J. *Macromolecules* 1991, **24**, 6182
16 Lowenhaupt, B. and Hellmann, G. P. *Polymer* 1991, **32**, 1065
17 Tanaka, H., Hasegawa, H. and Hashimoto, T. *Macromolecules* 1991, **24**, 240
18 Mayes, A. M., Russell, T. P., Satija, S. K. and Majkrzak, C. F. *Macromolecules* 1992, **25**, 6523
19 Jeon, K. J. and Roe, R. J. *Macromolecules* 1994, **27**, 2439
20 Koizumi, S., Hasegawa, H. and Hashimoto, T. *Macromolecules* 1994, **27**, 4371
21 Meier, D. J. *Polymer Prepr., Div. Polym. Chem., ACS* 1977, **18**, 340
22 Leibler, L., Orland, H. and Wheeler, J. C. *Macromolecules* 1983, **18**, 3550
23 Whitmore, M. D. and Noolandi, J. *Macromolecules* 1985, **18**, 2486
24 Roe, R. J. and Zin, W.-Ch. *Macromolecules* 1984, **17**, 189
25 Mayes, A. M. and de la Cruz, M. O. *Macromolecules* 1988, **21**, 2543
26 Kinning, D. J., Winey, K. I. and Thomas, E. L. *Macromolecules* 1988, **21**, 3502
27 Kinning, D. J., Thomas, E. L. and Fetters, L. J. *J. Chem. Phys.* 1989, **90**, 5806
28 Thomas, E. L. *Proc. ACS Div. Polym. Mater. Sci. Eng.* 1990, **62**, 686
29 Winey, K. I., Thomas, E. L. and Fetters, L. J. *J. Chem. Phys.* 1991, **95**, 9367
30 Winey, K. I., Thomas, E. L. and Fetters, L. J. *Macromolecules* 1992, **25**, 2645
31 Tucker, P. S. and Paul, D. R. *Macromolecules* 1988, **21**, 2801
32 Tucker, P. S., Barlow, J. W. and Paul, D. R. *Macromolecules* 1988, **21**, 1678, 2794
33 Brown, H. R., Char, K. and Deline, V. R. *Macromolecules* 1990, **23**, 3383
34 Hashimoto, T., Kimishima, K. and Hasegawa, H. *Macromolecules* 1991, **24**, 5704
35 Akiyama, M. and Jamieson, A. M. *Polymer* 1992, **33**, 3582
36 Auschar, C., Stadler, R. and Voigt-Martin, I. G. *Polymer* 1993, **34**, 2094
37 Lowenhaupt, B., Steurer, A., Hellmann, G. P. and Gallot, Y. *Macromolecules* 1995, **27**, 908
38 Adedeji, A., Jamieson, A. M. and Hudson, S. D. *Polymer* 1995, **36**, 2743
39 Adedeji, A., Hudson, S. D. and Jamieson, A. M. *Macromolecules* 1996, **29**, 2449
40 Tanaka, H. and Hashimoto, T. *Polym. Commun.* 1988, **29**, 212
41 Kinning, D. J., Thomas, E. L. and Fetters, L. J. *Macromolecules* 1991, **24**, 3893
42 Amundson, K., Helfand, E., Sanjay, P., Xina, Q. and Smith, S. D. *Macromolecules* 1992, **25**, 1935
43 Flory, P. J. 'Statistical Mechanics of Chain Molecules', Hanser, New York, 1989, p. 40
44 Braun, H., Rudolf, B. and Cantow, H. J. *Polym. Bull.* 1994, **32**, 241
45 Adedeji, A., Hudson, S. D. and Jamieson, A. M. *Polymer Commun.* (in press)
46 Sato, T., Tsujita, Y., Takizawa, A. and Kinoshita, T. *Macromolecules* 1991, **24**, 158